Accepted Manuscript

Two functionally distinct CYP4G genes of *Anopheles gambiae* contribute to cuticular hydrocarbon biosynthesis

Mary Kefi, Vasileia Balabanidou, Vassilis Douris, Gareth Lycett, René Feyereisen, John Vontas

A

An. gambiae pupal oenocytes

larval origin

non-cytoplasmic

PM

4G17   4G16

cytoplasmic

ER

adult origin

non-cytoplasmic

PM

4G16

cytoplasmic

★

4G17

ER

B

4G1

NO ECLOSION

| 4G1 WT | 4G17 ➕ | 4G17 ➕ | 4G16 ➕ | 4G16 ➕ | 4G16 ➕ | 4G17 ➕ |
| 93% | 33% | | 86% | | 83% | SURVIVAL |

Not found in CYP4G1

CHCs Relative abundance

dimethyl C45   dimethyl C46   dimethyl C47

1 **Two functionally distinct CYP4G genes of *Anopheles gambiae***
2 **contribute to cuticular hydrocarbon biosynthesis**

3

4 **Mary Kefi[a,b], Vasileia Balabanidou[a], Vassilis Douris[a], Gareth Lycett[c], René**
5 **Feyereisen[d], John Vontas[a,d,*]**

6

7 [a]Institute of Molecular Biology and Biotechnology, Foundation for Research and
8 Technology-Hellas, 73100 Heraklion, Greece

9 [b]Department of Biology, University of Crete, VassilikaVouton, 71409, Heraklion,
10 Greece

11 [c]Department of Vector Biology, Liverpool School of Tropical Medicine, Liverpool L3
12 5QA, United Kingdom;

13 [d]Department of Plant and Environmental Sciences, University of Copenhagen,
14 Copenhagen, 1017, Denmark.

15 [d]Pesticide Science Laboratory,Department of Crop Science, Agricultural University of
16 Athens, 11855 Athens, Greece

17

18

19 *Corresponding author: J. Vontas (vontas@imbb.forth.gr)

20

21
22

23

Abstract

25

26 Cuticular hydrocarbon (CHC) biosynthesis is a major pathway of insect physiology.

27 In *Drosophila melanogaster* the cytochrome P450 CYP4G1 catalyses the insect-

28 specific oxidative decarbonylation step, while in the malaria vector *Anopheles*

29 *gambiae*, two CYP4Gs paralogues, CYP4G16 and CYP4G17 are present. Analysis of

30 the subcellular localization of CYP4G17 and CYP4G16 in larval and pupal stages

31 revealed that CYP4G16 preserves its PM localization across developmental stages

32 analyzed; however CYPG17 is differentially localized in two distinct types of pupal

33 oenocytes, presumably oenocytes of larval and adult developmental specificity.

34 Western blot analysis showed the presence of two CYP4G17 forms, potentially

35 associated with each oenocyte type. Both *An. gambiae CYP4G*s were expressed in *D.*

36 *melanogaster* flies in a *Cyp4g1* silenced background in order to functionally

37 characterize them *in vivo*. *CYP4G16*, *CYP4G17* or their combination rescued the

38 lethal phenotype of *Cyp4g1*-knock down flies, demonstrating that CYP4G17 is also a

39 functional decarbonylase, albeit of somewhat lower efficiency than CYP4G16 in

40 *Drosophila*. Flies expressing mosquito CYP4G16 and/or CYP4G17 produced similar

41 CHC profiles to 'wild-type' flies expressing the endogenous CYP4G1, but they also

42 produce very long-chain dimethyl-branched CHCs not detectable in wild type flies,

43 suggesting that the specificity of the CYP4G enzymes contributes to determine the

44 complexity of the CHC blend. In conclusion, both *An. gambiae* CYP4G enzymes

45 contribute to the unique *Anopheles* CHC profile, which has been associated to

46 defense, adult desiccation tolerance, insecticide penetration rate and chemical

47 communication.

48
49
50
51 Keywords: *Anopheles gambiae,* CYP4Gs, P450 decarbonylase, oenocytes, cuticular

52 hydrocarbons (CHCs)

53

2

54

1. INTRODUCTION

Insect cuticular hydrocarbons (CHCs) are a complex blend of long-chain alkanes or alkenes and methyl-branched alkanes that act as essential waterproofing components of the insect epicuticular layer to prevent desiccation, and/or serve as species- and sex-specific semiochemicals (Arcaz et al., 2016; Chung and Carroll, 2015; Cocchiararo-Bastias et al., 2011; Gibbs, 2011; Howard and Blomquist, 2005). Although CHC profiles differ among insect species, the main biosynthetic pathway is conserved (Howard and Blomquist, 2005). Their synthesis from fatty acids requires a suite of elongases, desaturases and acyl-CoA reductases that function in concert in large, ectodermally derived cells, called oenocytes (Fan et al., 2003). An additional enzyme required for the final step of CHC synthesis, a cytochrome P450 of the CYP4G subfamily was identified as oxidative decarbonylase (Qiu et al., 2012). *Drosophila* CYP4G1 is highly expressed in oenocytes together with NADPH cytochrome P450 reductase (CPR) and catalyzes the oxidative decarbonylation of long-chain aldehydes (Qiu et al., 2012). Oenocyte-specific RNAi-mediated knock down of CYP4G1 results in severe susceptibility to desiccation, conferring high mortality at emergence (Qiu et al., 2012). The CYP4G P450 subfamily is evolutionarily conserved across insects (Feyereisen, 2006) but is absent in other orders, such as crustaceans and chelicerates. This may indicate an essential function of *CYP4G* genes specific to insects, suggested to be a key to success in terrestrial adaptation. Insect genomes sequenced so far possess at least one CYP4G (one in honey bee and aphid, two in *Drosophila* and several mosquito species) (Qiu et al., 2012).

Several earlier studies indicate distinct lipid/CHC signatures across development. Firstly, the necessary renewal of the cuticular lipids at each molt (Wigglesworth, 1988) implies distinct lipids and presumably differences in their CHC derivatives at different developmental stages. Secondly, aquatic insects should prevent liquid entry into the tracheal system while apart from this terrestrial insects must be protected from desiccation which means they should prevent water loss. Adult *An. gambiae* and *D. melanogaster* with their early developmental stages being aquatic or semi-aquatic respectively (Parvy et al., 2012) presumably reflect the distinct needs in

86   lipids/hydrocarbons through development. Larval oenocytes synthesize very-long-

87   chain fatty acids (VLCFA) which are accumulated into spiracles, the organs

88   controlling the entry of air into the trachea, protecting respiratory system from liquid

89   entry (Parvy et al., 2012). Oenocyte-specific RNAi-based knock down of *Cyp4g1* or

90   *Cpr* in larvae and adults results in severe depletion in epicuticular HC in the few adult

91   survivors. The majority die at eclosion presumably of extreme sensitivity to

92   desiccation at the time of adult emergence (Qiu et al., 2012). Furthermore,

93   pheromone-driven courtship was altered in *Cyp4g1*-KD CHC depleted females (Qiu

94   et al., 2012). Similar phenotypes are produced when oenocytes are specifically ablated

95   in adult *Drosophila* females.

96   Underlying this phenotype is the presence of two different oenocyte cells in larvae

97   and adults that have separate developmental origins (Billeter et al., 2009; Gutierrez et

98   al., 2007; Makki et al., 2014) and have been described in mosquitoes (Lycett et al.,

99   2006) and other Diptera (Makki et al., 2014). Overall, these latter studies suggest that

100 presumably larval oenocytes have a primary role in CHC production during molting

101 and water-loss prevention in the tracheal system, while CHCs produced from adult

102 oenocytes are mostly implicated in sex- and species-specificity, pheromonal

103 communication and desiccation resistance (Makki et al., 2014; Parvy et al., 2012).

104 The fact that *An. gambiae* oenocytes express two CYP4Gs (CYP4G16 and CYP4G17)

105 as opposed to the single CYP4G expressed in *D. melanogaster* oenocytes is possibly

106 indicative of a functional diversity. A recent study has shown that CYP4G16 is bound

107 on the periphery of adult oenocytes, while CYP4G17 is dispersed among the

108 cytoplasm (Balabanidou et al., 2016). In addition, *in vitro* experiments indicate the

109 ability of CYP4G16 to catalyze the conversion of long-chain aldehydes to

110 hydrocarbons, hence completing the final biosynthetic step, whereas the role of

111 CYP4G17 remains unknown (Balabanidou et al., 2016). While CYP4G16 was able to

112 convert C18 aldehyde to HC, no such activity could be demonstrated for CYP4G17

113 which did not express well *in vitro* and for which longer aldehydes could not be tested

114 because of solubility issues (Balabanidou et al., 2016). A recent study in

115 *Dendroctonus ponderosae* showed that shorter-chain alcohols can also be substrates

4

116   of CYP4Gs (MacLean et al., 2018), which can thus serve in the biosynthesis of the

117   pine beetle pheromone exo-brevicomin as well as in CHC biosynthesis.

118   The variation in insect CHC blend has been associated with physiological adaption to

119   ecological and reproductive parameters (Chung and Carroll, 2015). Indeed, methyl-

120   branched CHCs have been shown to affect both waterproofing and mating in

121   *Drosophila serrata* (Chung et al., 2014). It is likely that longer carbon chains in CHCs

122   increase the melting temperature of the insect epicuticular wax layer and probably

123   influence desiccation resistance, and methyl branching increases the chemical

124   information of the cuticle (Chung and Carroll, 2015). Some studies have indicated

125   that *An. gambiae* is rich in methyl-branched very long chain CHCs (mono- or

126   dimethyl) (Balabanidou et al., 2016; Caputo et al., 2005), which could potentially

127   serve both biological functions.

128   Moreover, cuticular analysis of an insecticide resistant *An. gambiae* population

129   compared to a susceptible one, revealed a thicker epicuticle, the major deposition site

130   of CHCs, in the femur leg segment, thus creating a thicker hydrophobic barrier to

131   insecticide molecules, as shown by reduced penetration rate of radiolabeled

132   insecticide (Balabanidou et al., 2016). The higher CHC amount is in line with the

133   overexpression of CYP4Gs in the resistant mosquitoes (Balabanidou et al., 2016),

134   implicating an additional role of CHCs in insecticide penetration resistance

135   (Balabanidou et al., 2018).

136   In this study, the subcellular localization of *An. gambiae* CYP4Gs was analyzed in

137   oenocytes from earlier developmental stages, i.e. 4th instar larvae and pupae.

138   Furthermore, functional analysis of the *An. gambiae* CYP4Gs was performed *in vivo*

139   using GAL4/UAS heterologous expression coupled with RNAi knock-down of the

140   endogenous *Cyp4g1* gene in *Drosophila melanogaster* and the ability of CYP4G16

141   and/or CYP4G17 in different doses and in combination to rescue the lethal (*Cyp4g1*

142   Knock-down) phenotype. CHC analysis of the rescued flies then gave insights into the

143   catalytic efficiency and specificity of the two anophelinae Cyp4Gs in a *Drosophila*

144   background.

145   **2. MATERIALS AND METHODS**

146   *2.1 Mosquito strains*

147   The *An. gambiae* N'Gousso strain was reared under standard insectary conditions at

148   27°C and 70-80% humidity under a 12:12 hour photoperiod. The strain is originally

149   from Cameroon and it is susceptible to all classes of insecticide (Edi et al., 2012).

150   *2.2 Antibodies*

151   Rabbit polyclonal antibodies targeting CYP4G16 have previously been developed

152   (Balabanidou et al., 2016). The specific antibodies that were used for the detection of

153   CYP4G17 (AGAP000877) have previously been described (Ingham et al., 2014). The

154   epitopes recognize residues 231-312 and 233-315 of CYP4G16 and CYP4G17

155   respectively.

156   *2.3 Preparation of cryosections for immunohistochemistry, immunofluorescence and*

157   *microscopy*

158   4th instar *An. gambiae* larvae and dissected pupal abdomens were fixed in cold

159   solution of 4% PFA (methanol free, Thermo scientific) in phosphate-buffered saline

160   (PBS) for 4 h, cryo-protected in 30% sucrose/PBS at 4° C for 12 h, immobilized in

161   Optimal Cutting Temperature O.C.T. (Tissue-Tek, SAKURA) and stored at -80°C

162   until use. Immunofluorescence analysis, followed by confocal microscopy, was

163   performed on longitudinal sections of the frozen larval and pupal specimens as

164   described previously (Ingham et al., 2014). Briefly, 7 μm sections, obtained in

165   cryostat with UVC disinfection (Leica CM1850UV) were washed (3 x 5 min) with

166   0,05% Tween in PBS and blocked for 3 h in blocking solution (1% Fetal Bovine

167   Serum, biosera, in 0,05% Triton/PBS). Then, the sections were stained with rabbit

168   primary antibodies in 1/500 dilution, followed by goat anti-rabbit (Alexa Fluor 405,

169   Molecular Probes) (1/1000) that gave the cyan color. Also To-PRO 3-Iodide

170   (Molecular Probes), which specifically stains DNA (red color), was used, after

171   RNAse A treatment. Finally, images were obtained on a Leica SP8 laser-scanning

172   microscope, using the 40-objective.

173

174   *2.4 Topology experiments: predictions and whole mounts (preparation of abdominal*

175   *walls for immunohistochemistry and immunofluorescence)*

176 The predicted membrane topology of both *An. gambiae* CYP4Gs was analyzed using

177 Phobius, a transmembrane topology and signal peptide predictor program (Kall et al.,

178 2007). For whole-mount larval abdomen immunostaining, abdominal walls from 4th

179 instar larvae were dissected and fixed for 30 min at room temperature in 4%

180 methanol-free formaldehyde (Thermo Scientific) in PBS supplemented with 2 mM

181 $MgSO_4$ and 1 mM EGTA, washed for 5 min with PBS, and then washed with

182 methanol for precisely 2 min. After methanol wash, the tissues were washed again

183 with PBS and then blocked for 1 h in blocking solution (bl sol: 1% BSA, 0.1% Triton

184 X-100 in PBS). Then the tissues were stained with rabbit primary antibodies in 1/500

185 dilution in the blocking solution, followed by goat anti-rabbit antibody (Alexa-Fluor

186 488; Molecular Probes; 1:1,000) that gave the green color. Up to this point the same

187 protocol omitting the addition of Triton was used to create the non-permeabilized

188 conditions. Finally, DNA was stained red with ToPRO 3-Iodide (Molecular Probes).

189 Pictures were obtained on Leica M205 FA Fluorescent Stereomicroscope.

190 *2.5 Fly strains*

191 In order to drive oenocyte –specific expression, the RE-Gal4 driver line ((Bousquet et

192 al., 2012); kindly provided by Jean-Francois Ferveur, Université de Bourgogne,

193 Dijon, France) was employed. This line contains the RE fragment of the *desat1* gene

194 promoter, whose expression is mostly confined to oenocytes in *Drosophila* adults,

195 (though some expression is also observed in accessory glands in males (Bousquet et

196 al., 2012)). The responder strain UAS-Cyp4g1-KD (#102864 KK from Vienna

197 Drosophila Resource Center) was used for RNAi mediated knock-down of CYP4G1.

198 *2.6 Generation of UAS responder flies*

199 Since both the RE-Gal4 driver and UAS-Cyp4g1-KD responder transgenes are

200 located on *Drosophila* chromosome 2, the two 'mosquito CYP4G' responder fly

201 strains were generated by φC31 integrase mediated attB insertion (Groth et al., 2004)

202 using landing site VK13 in chromosome 3 to facilitate downstream manipulations.

203 Two *ad hoc* integration vectors were generated by modifying the vector

204 dPelican.attB.UAS_CYP6A51 (Tsakireli et al., 2019). This plasmid is a modification

205 of a vector based on pPelican (Barolo et al., 2000) which contains *gypsy* insulator

206 sequences flanking the expression cassette (Piwko et al., 2019); plasmid #30)). Kapa

207 Taq DNA Polymerase (Kapa Biosystems) was used for the amplification of a 1713 bp

208 fragment containing *CYP4G16* ORF using primer pair CYP4G16F/CYP4G16R

209 (Table S1) that introduce a 5' BssHII site and a 3' XhoI site, while primer pair

210 CYP4G17F/CYP4G17R (Table S1) was used to amplify a 1711 bp fragment

211 containing the *CYP4G17* ORF and introducing a 5' AscI and a 3' SalI, respectively.

212 The templates for the amplification of CYP4G16 and CYP4G17 ORFs were cDNAs

213 of adult mosquito RNAs. PCR conditions were 95°C for 3 min, followed by 35 cycles

214 of 95°C for 30 sec, 50°C for 30 sec, 72 for 2 min. The amplicons were purified,

215 digested with the relevant enzyme combinations (BssHII/XhoI for *CYP4G16*

216 fragment and AscI/SalI for *CYP4G17* fragment) and subcloned into the unique

217 MluI/XhoI sites of dPelican.attB.UAS_CYP6A51 (Tsakireli et al., 2019) so that the

218 existing ORF is removed and replaced by the *CYP4G16* or *CYP4G17* ORFs

219 downstream of the 5xUAS-promoter sequence and just upstream of the SV40

220 polyadenylation sequence. Each *de novo* UAS expression recombinant plasmid

221 (dPelican.attB.UAS_CYP4G16 and dPelican.attB.UAS_CYP4G17) contained also a

222 mini-*white* marker for *Drosophila*. These plasmids were sequence verified using

223 primers pPel_uas F/pPel_sv40 R (Table S1) and used to inject preblastoderm embryos

224 of the *D. melanogaster* strain *y[1] M{vas-int.Dm}ZH-2A w[*]; PBac{y[+]-attP-*

225 *9A}VK00013* (referred hereafter as VK13 strain, #24864 in Bloomington Drosophila

226 Stock Center, kindly provided by M. Monastirioti and C. Delidakis, IMBB) which

227 enables φC31 integrase expression under *vasa* promoter in chromosome X and bears

228 an attP landing site in the 3rd chromosome. G_0 injected VK13 flies were crossed with

229 *yw* flies and G_1 progeny was screened for w[+] phenotypes (red eyes) indicating

230 integration of the recombinant plasmid. Independent transformed lines were crossed

231 with a balancer strain for the 3rd chromosome (*yw*; TM3 *Sb* / TM6B *Tb Hu*) and G_2

232 flies with red eyes and relevant marker phenotype were selected and crossed among

233 themselves to generate the homozygous flies used to establish the transgenic

234 responder lines (Figure S1).

235 *2.7 Generation of flies used for rescue experiment*

236 In order to generate flies where both oenocyte-specific *Drosophila* Cyp4g1 RNAi

237 knock-down and *Anopheles CYP4G16* and/or *CYP4G17* expression by one or two

238 transgene copies would take place, a series of standard genetic crosses (see Figure S1

239   for detailed strategy) was performed in order to generate homozygous lines bearing

240   either both RE-Gal4 (2nd chromosome) and UAS-*CYP4G16* or UAS-*CYP4G17* (3rd

241   chromosome), or both UAS-*Cyp4g1*-KD (2nd chromosome) and UAS-*CYP4G16* or

242   UAS-*CYP4G17* (3rd chromosome). Then, several different combinations of crosses

243   provided all the genotypes used for rescue experiments as shown in Table S2.

244   *2.8 Quantification of eclosion (adult survival and adult mortality)*

245   For quantification experiments appropriate fly crosses were set up by crossing 5

246   virgin females with 5 males of the appropriate genotypes as shown in Table S2. 2nd

247   instar larvae were collected and transferred into fly food in batches of 20

248   (approximately 130 larvae per biological replicate were transferred). Pupae were then

249   counted to determine pupation efficiency and successfully eclosed adults were

250   measured. To address eclosion we measured the alive adults (males and females),

251   while newly emerged adults that died immediately after eclosion were counted

252   separately in order to address the adult mortality, in three biological replicates.

253   *2.9 Extraction of cuticular lipids, Cuticular hydrocarbons (CHCs) Fractionation,*

254   *Identification and Quantitation.*

255   Crosses B x 2, B x 3, C x 3 and G x 1 (Table S2) were set up and the progeny (B2,

256   B3, C3 and G1, Table S2) was separated by sex at emergence. One-day old male flies

257   from each condition were dried in Room Temperature for at least 48 h.

258   Approximately 150 flies of each condition were separated in 3 replicates, the dry

259   weight of each replicate was measured and they were send for CHC analysis in

260   VITAS-Analytical Services (Oslo, Norway). Briefly, cuticular lipids from all samples

261   were extracted by 1-min immersion in hexane (x3) with gentle agitation; extracts were

262   pooled and evaporated under a N_2 stream. CHCs were separated from other

263   components and finally concentrated prior to chromatography by Solid Phase

264   Extraction (SPE). CHC identification by gas chromatography-mass spectrometry

265   (GC-MS) and CHC quantitation by GC-flame ionization detector (FID) were

266   performed as described previously (Balabanidou et al., 2016; Girotti et al., 2012).

267   Quantitative amounts were estimated by co-injection of nC24 as an internal standard

268   (2890ng/ml in hexane). CHC quantification was calculated as the sum of area of 32

269   peaks in total (peaks 3 and 4 were excluded due to background noise) and the relative

9

270 amount (mean value ± SD) of each component was calculated by dividing the

271 corresponding peak area by the total CHC peak area, using the internal standard.

272 Shorthand nomenclature of CHCs used in the text and tables is as follows: CXX

273 indicates the total number of carbons in the straight chain; linear alkanes are denoted

274 as n-CXX; the location of methyl branches is described as x-Me for monomethyl-

275 alkanes and as x,x-DiMe for dimethyl-alkanes. Alkenes are shown as x-CXX:1.

276 Statistics were analyzed using GraphPad Prism software, version 6.01. Differences in

277 the total CHC values were analyzed with Student's *t*-test.

278 *2.10 Western blots*

279 Abdominal walls from 4th instar larvae, 1-5 hour old pupae, 20-24 hour old pupae and

280 1-12 hour-old adults were homogenized into a Homogenization Buffer, containing 8

281 M Urea, 50 mM Tris-HCl, pH 8.0 and 0.5% SDS. Polypeptides resolved by SDS-

282 PAGE (10% acrylamide) were electro-transferred on nitrocellulose membrane (GE

283 Healthcare, Whatman) and probed with anti-CYP4G16, anti-CYP4G17 at a dilution

284 of 1:250 in TBS-Tween. Antibody binding was detected using goat anti-rabbit IgG

285 coupled to horseradish peroxidase (Cell Signaling) (diluted 1:10,000 in 1% skimmed

286 milk in TBS-Tween buffer), visualized using a horseradish peroxidase sensitive ECL

287 Western blotting detection kit (GE Healthcare, Little Chalfont, Buckinghamshire,

288 UK) and the result was recorded using Fujifilm LAS3000 CCD camera imaging

289 station.

290

291 **3. RESULTS**

292 *3.1. Both CYP4G17 and CYP4G16 are anchored on the plasma membrane of 4th*

293 *instar larval oenocytes with the globular part facing cytoplasmically.*

294 To determine the specific localization of CYP4G16 and CYP4G17 in 4th instar larvae,

295 an immunohistochemistry approach was employed. Longitudinal sections from frozen

296 pre-fixed mosquito specimens were immune-stained with anti-CYP4G17 and anti-

297 CYP4G16 specific antibodies, respectively. CYP4G16 and CYP4G17 antibodies gave

298 intense signals localizing in oenocytes. We were unable to detect specific signals in

299 other tissues by immune-staining. Surprisingly, higher magnification confocal

300 microscopy focusing on oenocytes revealed that both CYP4G17 and CYP4G16 are

301 found at the periphery of the larval oenocytes, presumably associated with the plasma

302 membrane (PM) (Figure 1). According to topology prediction tools both proteins were

303 predicted to have one transmembrane domain each. CYP4G16 and CYP4G17

304 transmembrane domains are predicted to span the residues seventeen to thirty nine

305 and twenty to forty one respectively. Hence, in order to investigate the hypothesis that

306 they span the membrane with one helix with the N-terminus located in the

307 extracellular space of oenocyte cells, separated from the remainder globular part of

308 the protein that is located intracellularly we performed immunohistochemical

309 experiments in abdominal larval walls in permeabilized and non-permeabilized

310 conditions (Figure 2). The fact that specific antibodies used recognize epitopes closer

311 to the C-termini of the proteins together with the absence of oenocyte-specific

312 staining in non-permeabilized conditions for both CYP4G16 and CYP4G17 as well as

313 *in silico* prediction strongly indicate that both are anchored on the plasma membrane,

314 facing the cytoplasm, with their N-termini residing outside of the cell.

315 *3.2 Two differentially localized CYP4G17 forms in pupal oenocytes, of larval and*

316 *adult origin.*

317 To immunolocalize CYP4G17 and CYP4G16 in pupae, the same

318 immunohistochemical approach in longitudinal cryosections in pupal abdominal walls

319 was performed as above. In pupa, both CYP4G16 and CYP4G17 antibodies gave

320 intense signals in two cell types. We detected both close to the lateral pupal cuticular

321 walls. The larger cells, full of round-shaped vesicular structures and lipid droplets are

322 the remaining larval oenocytes, while the smaller in size rounded-shaped cells that are

323 also found singly and in clusters are the newly-developing adult oenocytes (Figure 3).

324 CYP4G16 maintained a peripheral localization in both oenocyte types (Figure 3A and

325 B), whereas CYP4G17 antibody gave localized signals of two distinct patterns.

326 Peripheral staining (Figure 3C) was maintained in cells of larval origin, while the

327 developing adult cells were stained with anti-CYP4G17 throughout their cytoplasm

328 (Figure 3D).

329 To further examine the different sub-cellular localization observed in the two types of

330 oenocytes found in pupae, we performed western blot analysis with anti-CYP4G17

331 using abdominal walls of 4th instar larvae, newly-formed pupae (1-5 hour-old), pupae

11

332   prior to emergence (20-24 hour-old) and newly emerged adults (1-12 hour-old).

333   Interestingly, we observed two bands in different molecular sizes in all developmental

334   stages with a difference in the intensity in each condition tested (Figure 4). The lower

335   band has a molecular mass of around 65 kDa , which is close to the estimated

336   molecular mass of the protein (64 kDa), whereas the upper band migrates

337   approximately at 70 kDa.

338

339   *3.3 Oenocyte-specific expression of CYP4G16 and CYP4G17 in CYP4G1 knock-down*

340   *Drosophila can restore viability.*

341   Using a series of genetic manipulations we were able to induce the expression of

342   either or both mosquito CYP4Gs while simultaneously silencing the endogenous

343   *Cyp4g1* gene specifically in oenocytes (Figure S1 and Table S2). Phenotypic analysis

344   showed that all *Cyp4g1*-KD flies die at emergence, not being able to eclose from the

345   pupal case. However, viability was almost completely restored in the presence of two

346   copies of *CYP4G16* (with respective elevated transcripts 1.95 ±0.4 - fold, n=3,

347   p<0.01, compared to the single copy transgene flies) and of *CYP4G16* in combination

348   with *CYP4G17* (Figure S2). Quantitative analysis of all the different CYP4G

349   conditions tested revealed that CYP4G16 and CYP4G17 exhibit differential ability to

350   rescue the lethal phenotype in an oenocyte-specific *Cyp4g1*knock-down genetic

351   background (Figure 5). As shown in Figure 5, 86% of the larvae expressing *CYP4G16*

352   in two copies successfully emerged into adults, while *CYP4G17* in two copies is able

353   to rescue approximately 33% of the flies, revealing its ability to partially complement

354   *Cyp4g1* silencing. This demonstrates that CYP4G17 is also a functional oxidative

355   decarbonylase. The ability of each transgene to rescue the lethal phenotype is dose-

356   dependent since *CYP4G16* in one copy only partially restores viability (15%

357   survivors), while overexpression of one copy of *CYP4G17* seems to generate flies

358   arrested during eclosion. However, the combination of *CYP4G16* and *CYP4G17* gives

359   a high percentage of survivors (83%), similar to a double dose of *CYP4G16*.

360   Interestingly, in cases of partial rescue (1x *CYP4G16* or 2x *CYP4G17*), as well as in

361   the case of 1x *CYP4G17*, where no long time survivors are observed, a remarkable

362   number of newly-emerged adults, mostly females, survive the eclosion burden but die

363 almost immediately and are found lying dead on the food. This is in contrast to

364 *Cyp4g1*-KD flies where only dead adults unable to fully exit the puparium were

365 observed (Figures 5 and S2). Moreover, in partially rescued CYP4G backgrounds (1x

366 *CYP4G16* and 2x *CYP4G17*) the vast majority of successfully eclosed survivors

367 (almost 80%) are males.

368 *3.4. Three very long-chain dimethyl-branched CHCs are present in CYP4G16,*

369 *CYP4G17 and CYP4G16/CYP4G17 flies, but not 'wild-type' CYP4G1 flies*

370 After extraction of cuticular lipids and quantification, different total hydrocarbon

371 amounts were identified per mg of dry weight in each condition tested (Figure S3),

372 with the control flies (no knock-down of *Cyp4g1*) having the highest total CHC

373 content and the flies bearing the *CYP4G17* transgene in the absence of *Cyp4g1* the

374 lowest (p-value<0.001). CYP4G16/CYP4G17 and CYP4G16/CYP4G16 appeared to

375 have approximately the same total CHC amount (non-significant difference) (Figure

376 S3). Moreover, 18 CHC compounds were identified in the control flies (no mosquito

377 transgene) and 21 CHC compounds (18 similar and 3 extra) in the *D. melanogaster*

378 flies expressing mosquito transgenes. Interestingly, the three extra CHCs present in all

379 *Drosophila* strains expressing mosquito CYP4Gs but not in the control (CYP4G1)

380 flies, corresponded to the three longer CHCs (dimethyl-C45, dimethyl-C46 and

381 dimethyl-C47) identified (Figure 6) often found in *Anopheles*. Additionally, the

382 relative abundance of each CHC identified was calculated in % area and it was

383 showed that CYP4G17 and CYP4G16/CYP4G17 produce significantly more of these

384 three very-long chain methyl-branched compounds (Figure 6) than CYP4G16. Other

385 statistically significant differences indicate that C31 is more enriched in the presence

386 of CYP4G17 rather than CYP4G16 (p-value<0.001) and that C25 (p-value<0.0001),

387 C27 (p-value<0.0001), methyl-C29 (p-value<0.0001) and C31:1 (p-value<0.001) are

388 more abundant in CYP4G16 mosquitoes.

389
390 **4. DISCUSSION**
391

392 The CYP4G are highly conserved P450 enzymes in insects and the discovery that

393 they serve as oxidative decarbonylases in the last step of hydrocarbon biosynthesis

13

394 (Qiu et al., 2012) was the first explanation provided for this high degree of

395 conservation. However, much remains to be learned about these enzymes. In

396 *Drosophila*, CYP4G1 is a major protein of oenocytes, whereas its paralog CYP4G15

397 is found in the brain (Maibeche-Coisne et al., 2000) where its function is unknown. In

398 the major malaria vector *Anopheles gambiae* the situation is different, because both

399 the CYP4G1 and CYP4G15 paralogues, named CYP4G17 and CYP4G16 are highly

400 expressed in oenocytes (Balabanidou et al., 2016). This study further showed that

401 while a CPR-CYP4G16 fusion, was able to catalyze the oxidative decarbonylation of

402 a C18 aldehyde, this activity was not detectable for CYP4G17 (Balabanidou et al.,

403 2016). The two enzymes also differed in their subcellular localization in adult *An.*

404 *gambiae* oenocytes (Balabanidou et al., 2016). The results presented here address both

405 differences between CYP4G16 and CYP4G17.

406 In contrast to that expected for microsomal P450s, CYP4G16 was previously shown

407 to be present on the internal side of the PM in adult oenocytes (Balabanidou et al.,

408 2016) and here we show that it has the same subcellular localization and topology in

409 oenocytes from an earlier developmental stage and origin (Figures 1B, 3A, 3B). In

410 larval oenocytes, CYP4G17 also appears anchored to the PM (Figure 1A and 3C).

411 The N-terminus of each protein is predicted to be facing extracellularly with a

412 transmembrane helix connecting to the catalytic part of the enzyme, shown to be on

413 the cytoplasmic side (Figure 2). In pupae, CYP4G17 is found to be dispersed

414 throughout the cytoplasm in developing adult-type oenocytes (Figures 3D) as we have

415 observed previously in fully developed adults (Balabanidou et al., 2016). This

416 difference in CYP4G17 localization is also accompanied by a difference in molecular

417 weight, as indicated by western blot analysis of different developmental stages

418 (Figure 4). One plausible scenario is that the two bands identified in Figure 4

419 represent developmentally specific isoforms; under this scenario adult CYP4G17

420 (*ad*CYP4G17) may be modified by a yet unidentified pre- or post-translational

421 mechanism, sufficient for the protein to be rendered to the ER as a typical ER-resident

422 P450, while larval CYP4G17 (*lar*CYP4G17) escapes the ER-rendering mechanism

423 and is transported to the PM. Genomic sequence and transcript analysis does not

424 indicate obvious alternative splicing, so we favor a post-translational modification

425 that may be confirmed by proteomic analysis in future work. Under this hypothesis

14

426 *lar* or *ad*CYP4G17 may also be functionally distinct. It is tempting to suggest that PM

427 localization would favor export of CHC from the cell and transfer to lipophorin.

428 However nothing is known yet of the physiology of intracellular CHC transport, and

429 the localization of the upstream enzymes in oenocytes, desaturases and elongases, has

430 been predicted but not verified.

431 The hypothesis of two different CYP4G17 isoforms is in line with the observation

432 that the two different types of oenocytes co-exist in the mosquito pupa. It is known

433 that in *D. melanogaster*, larval and adult generations of oenocytes are

434 morphologically distinct ectodermal derivatives with separate developmental origins

435 (Makki et al., 2014). In *An. gambiae* two distinct types of oenocytes have previously

436 been found in larvae and adults stained for cytochrome P450 reductase (Lycett et al.,

437 2006). Oenocyte functions seem to be closely related with molting, as a new

438 generation of such cells is developed at each molt in some holometabolous species

439 and the size and number of these cells can vary dramatically during *Drosophil*a larval

440 development (Makki et al., 2014). Under our immunostaining approach in pupal

441 abdomens, CYP4G17 and CYP4G16 oenocyte-specific intense staining revealed the

442 morphological difference of oenocytes forms at this stage. Two distinct cell types that

443 had similar morphologies to those described previously in larvae (Lycett et al., 2006)

444 and adults (Balabanidou et al., 2016; Lycett et al., 2006) were found in pupae

445 probably owing to the existence of two different origins of oenocytes in the pupal

446 developmental stage. Big cells in size, carrying numerous bundles of lipid droplets are

447 considered to be oenocytes of larval origin persisting in the pupal stage as they are

448 very similar to those obtained in larvae longitudinal sections (Figure 3A and C). Apart

449 from these intense specific staining was obtained in smaller in size cells also found in

450 clusters that are considered to be newly-developing oenocytes of adult-specificity

451 (Figure 3B and D).

452 Our previous biochemical analysis could not detect decarbonylase activity of

453 CYP4G17on short chain aldehydes, and so we have examined the comparative

454 functions of the CYP4Gs by a genetic, *in vivo* approach. In this study, we performed

455 the conditional expression of *An. gambiae* CYP4Gs in oenocytes of *Cyp4g1* knock-

456 down *D. melanogaster* flies, in order to investigate if this expression could rescue the

457 knock-down phenotype. Our results revealed that two copies of *CY4G16* or a

458 *CYP4G16/CYP4G17* combination can almost completely restore the viability of

459 *Cyp4g1*-KD flies, while one copy of CYP4G16 and two copies of *CYP4G17*only lead

460 to a partial rescue, indicating that both mosquito CYP4Gs can functionally substitute

461 the fly decarbonylase, albeit to a different extent. Interestingly 1x *CYP4G17* showed

462 almost zero levels of adult survival although a remarkable number of dead, early-

463 emerged adults were found lying on the food in contrast to control *Cyp4g1*-KD flies

464 (Figure 5 and S2), which could not fully exit the puparium , implying that even the

465 slight expression of CYP4G17(one allele present) results in better eclosion ability.

466 The results show that gene copy number (i.e. dose) affects survival ability. This is

467 consistent with the very high expression level of native oenocyte CYP4Gs

468 (Balabanidou et al., 2016; Chung et al., 2009), the sluggish enzyme activity observed

469 *in vitro* until now (Balabanidou et al., 2016; Calla et al., 2018; Qiu et al., 2012) and

470 the potentially lower level of activation provided by the RE driver. Interestingly, in

471 cases of partial rescue (2x *CYP4G17* and 1x *CYP4G16*), males preferentially survive.

472 Several studies on *Drosophila* species from temperate and tropical regions have

473 shown a higher desiccation resistance of females than males (Parkash and Ranga,

474 2013). Perhaps, if females require more CHC for desiccation resistance, a deficit is

475 more difficult to compensate. Alternatively, this may be the result of subtle

476 differences in expression levels or spatiotemporal profile of the RE-Gal4 driver

477 (Bousquet et al., 2012) between males and females that may affect CYP4G1 knock-

478 down efficiency or specificity.

479 Since both *Anopheles* CYP4Gs can function as decarbonylases, we investigated the

480 cuticular hydrocarbon profile of 'rescued' flies where CYP4G1 native expression in

481 oenocytes has been knocked down and functionally substituted with one or both of the

482 mosquito genes. In *Drosophila* oenocytes, CYP4G1 is the only oxidative

483 decarbonylase, so the blend of CHC produced reflects the catalytic activity of a single

484 enzyme on a large number of substrates that differ in length, saturation, and methyl

485 branching. Its substrate specificity must therefore be quite broad. In the rescued flies,

486 the total amount of hydrocarbons produced was somewhat lower than wild type.

487 However, the pattern of hydrocarbons produced in flies rescued with alternative

488 *Anopheles* 4Gs was different, indicating that the CYP4G enzymes may have a

489 different substrate specificity to each other, and to the CYP4G1. In particular, three

490 extra CHCs (dimethyl alkanes of very high MW) were detected in all cases where

491 mosquito CYP4Gs (but not *Drosophila* CYP4G1) were present. These higher MW

492 compounds are typically found on the *An. gambiae* cuticle (Balabanidou et al., 2016).

493 The substrates for CYP4G enzymes are produced by a complex pathway of enzymes

494 (ACCase, elongases, desaturases, acyl-CoA reductases), encoded by a large number

495 of genes (Wicker-Thomas et al., 2015). It is the flux through those enzymes that

496 determines the substrate pool for the CYP4G enzymes. Transport in the hemolymph

497 (on lipophorins) and then through the epidermis and differential loss from the

498 epicuticle then determines the blend of CHC that is measured. It is intriguing how

499 these processes contribute to the apparition of higher MW CHCs not detected in wild

500 type *Drosophila*. Although speculative, we propose several non-exclusive factors to

501 explain this novel observation. On one hand, it is entirely plausible that the dimethyl-

502 C45, -46 and -47 substrates are produced and converted to CHC in wild type

503 *Drosophila* oenocytes at a level below detection in our assay. Indeed the classical GC

504 method detects high MW CHC poorly and other methods are needed (Cvacka et al.,

505 2006). On the other hand, in transgenic flies these substrates may be more efficiently

506 converted by CYP4G16 and especially CYP4G17 than by CYP4G1. By drawing on

507 the pool of high MW substrates, CYP4G17 (and CYP4G16) would increase their

508 synthesis by relieving product inhibition of the Elovl elongases. Thus, more high MW

509 substrates would become available in the transgenic flies than in the wild type flies.

510 Furthermore, greater retention of the high MW CHC has been noted before (Qiu et al.,

511 2012) so that both biochemical processes may contribute to the presence of dimethyl-

512 C45, -46 and -47 alkanes in transgenic flies and allow their detection by our classical

513 method. Our study therefore suggests that it is not only the activities of upstream

514 enzymes in oenocytes that determines the blend of insect CHC (Qiu et al., 2012), but

515 that substrate specificity of the last enzymes, the CYP4Gs, also contributes to it. This

516 conclusion reaffirms the need to delineate CYP4G specificity, especially in insects

517 that express more than one CYP4G gene in oenocytes.

518 Furthermore, the differential subcellular localization of CYP4G17 during

519 development and its apparent ability to act as a more efficient decarbonylase of very

520 long-chain dimethyl-branched compounds in *Drosophila* reveal an intriguing

521 functional diversification of the *An. gambiae* CYP4Gs. Further studies will be aimed

522 to elucidate the molecular mechanisms of differential localization of CYP4G17 in

523 larval and adult oenocytes, and to delineate precisely the substrate specificity of each

524 CYP4G enzyme.

525

526

545

546 **5. REFERENCES**

547

548 Arcaz, A.C., Huestis, D.L., Dao, A., Yaro, A.S., Diallo, M., Andersen, J., Blomquist,
549 G.J., Lehmann, T., 2016. Desiccation tolerance in Anopheles coluzzii: the effects of
550 spiracle size and cuticular hydrocarbons. J Exp Biol 219, 1675-1688.
551 Balabanidou, V., Grigoraki, L., Vontas, J., 2018. Insect cuticle: a critical determinant
552 of insecticide resistance. Curr Opin Insect Sci 27, 68-74.

553 Balabanidou, V., Kampouraki, A., MacLean, M., Blomquist, G.J., Tittiger, C., Juarez,
554 M.P., Mijailovsky, S.J., Chalepakis, G., Anthousi, A., Lynd, A., Antoine, S.,
555 Hemingway, J., Ranson, H., Lycett, G.J., Vontas, J., 2016. Cytochrome P450
556 associated with insecticide resistance catalyzes cuticular hydrocarbon production in
557 Anopheles gambiae. Proc Natl Acad Sci U S A 113, 9268-9273.
558 Barolo, S., Carver, L.A., Posakony, J.W., 2000. GFP and beta-galactosidase
559 transformation vectors for promoter/enhancer analysis in Drosophila. Biotechniques
560 29.
561 Billeter, J.C., Atallah, J., Krupp, J.J., Millar, J.G., Levine, J.D., 2009. Specialized
562 cells tag sexual and species identity in Drosophila melanogaster. Nature 461, 987-991.
563 Bousquet, F., Nojima, T., Houot, B., Chauvel, I., Chaudy, S., Dupas, S., Yamamoto,
564 D., Ferveur, J.F., 2012. Expression of a desaturase gene, desat1, in neural and
565 nonneural tissues separately affects perception and emission of sex pheromones in
566 Drosophila. Proc Natl Acad Sci U S A 109, 249-254.
567 Calla, B., MacLean, M., Liao, L.H., Dhanjal, I., Tittiger, C., Blomquist, G.J.,
568 Berenbaum, M.R., 2018. Functional characterization of CYP4G11-a highly conserved
569 enzyme in the western honey bee Apis mellifera. Insect Mol Biol 27, 661-674.
570 Caputo, B., Dani, F.R., Horne, G.L., Petrarca, V., Turillazzi, S., Coluzzi, M.,
571 Priestman, A.A., della Torre, A., 2005. Identification and composition of cuticular
572 hydrocarbons of the major Afrotropical malaria vector Anopheles gambiae s.s.
573 (Diptera: Culicidae): analysis of sexual dimorphism and age-related changes. J Mass
574 Spectrom 40, 1595-1604.
575 Chung, H., Carroll, S.B., 2015. Wax, sex and the origin of species: Dual roles of
576 insect cuticular hydrocarbons in adaptation and mating. Bioessays 37, 822-830.
577 Chung, H., Loehlin, D.W., Dufour, H.D., Vaccaro, K., Millar, J.G., Carroll, S.B.,
578 2014. A single gene affects both ecological divergence and mate choice in
579 Drosophila. Science 343, 1148-1151.
580 Chung, H., Sztal, T., Pasricha, S., Sridhar, M., Batterham, P., Daborn, P.J., 2009.
581 Characterization of Drosophila melanogaster cytochrome P450 genes. Proc Natl Acad
582 Sci U S A 106, 5731-5736.
583 Cocchiararo-Bastias, L.M., Mijailovsky, S.J., Calderon-Fernandez, G.M., Figueiras,
584 A.N., Juarez, M.P., 2011. epicuticle lipids mediate mate recognition in Triatoma
585 infestans. Journal of chemical ecology 37, 246-252.
586 Cvacka, J., Jiros, P., Sobotnik, J., Hanus, R., Svatos, A., 2006. Analysis of insect
587 cuticular hydrocarbons using matrix-assisted laser desorption/ionization mass
588 spectrometry. J Chem Ecol 32, 409-434.
589 Edi, C.V.A., Koudou, B.G., Jones, C.M., Weetman, D., Ranson, H., 2012. Multiple-
590 Insecticide Resistance in Anopheles gambiae Mosquitoes, Southern Cote d'Ivoire.
591 Emerging infectious diseases 18, 1508-1511.
592 Fan, Y., Zurek, L., Dykstra, M.J., Schal, C., 2003. Hydrocarbon synthesis by
593 enzymatically dissociated oenocytes of the abdominal integument of the German
594 Cockroach, Blattella germanica. Die Naturwissenschaften 90, 121-126.
595 Feyereisen, R., 2006. Evolution of insect P450. Biochemical Society transactions 34,
596 1252-1255.
597 Gibbs, A.G., 2011. Thermodynamics of cuticular transpiration. Journal of Insect
598 Physiology 57, 1066-1069.
599 Girotti, J.R., Mijailovsky, S.J., Juarez, M.P., 2012. Epicuticular hydrocarbons of the
600 sugarcane borer Diatraea saccharalis (Lepidoptera: Crambidae). Physiological
601 Entomology 37, 266-277.

602 Groth, A.C., Fish, M., Nusse, R., Calos, M.P., 2004. Construction of transgenic
603 Drosophila by using the site-specific integrase from phage phiC31. Genetics 166,
604 1775-1782.
605 Gutierrez, E., Wiggins, D., Fielding, B., Gould, A.P., 2007. Specialized hepatocyte-
606 like cells regulate Drosophila lipid metabolism. Nature 445, 275-280.
607 Howard, R.W., Blomquist, G.J., 2005. Ecological, behavioral, and biochemical
608 aspects of insect hydrocarbons. Annu Rev Entomol 50, 371-393.
609 Ingham, V.A., Jones, C.M., Pignatelli, P., Balabanidou, V., Vontas, J., Wagstaff, S.C.,
610 Moore, J.D., Ranson, H., 2014. Dissecting the organ specificity of insecticide
611 resistance candidate genes in Anopheles gambiae: known and novel candidate genes.
612 BMC genomics 15, 1018.
613 Kall, L., Krogh, A., Sonnhammer, E.L., 2007. Advantages of combined
614 transmembrane topology and signal peptide prediction--the Phobius web server.
615 Nucleic Acids Res 35, 5.
616 Lycett, G.J., McLaughlin, L.A., Ranson, H., Hemingway, J., Kafatos, F.C., Loukeris,
617 T.G., Paine, M.J., 2006. Anopheles gambiae P450 reductase is highly expressed in
618 oenocytes and in vivo knockdown increases permethrin susceptibility. Insect Mol Biol
619 15, 321-327.
620 MacLean, M., Nadeau, J., Gurnea, T., Tittiger, C., Blomquist, G.J., 2018. Mountain
621 pine beetle (Dendroctonus ponderosae) CYP4Gs convert long and short chain
622 alcohols and aldehydes to hydrocarbons. Insect Biochem Mol Biol 102, 11-20.
623 Maibeche-Coisne, M., Monti-Dedieu, L., Aragon, S., Dauphin-Villemant, C., 2000. A
624 new cytochrome P450 from Drosophila melanogaster, CYP4G15, expressed in the
625 nervous system. Biochem Biophys Res Commun 273, 1132-1137.
626 Makki, R., Cinnamon, E., Gould, A.P., 2014. The development and functions of
627 oenocytes. Annu Rev Entomol 59, 405-425.
628 Parkash, R., Ranga, P., 2013. Sex-specific divergence for adaptations to dehydration
629 stress in Drosophila kikkawai. J Exp Biol 216, 3301-3313.
630 Parvy, J.P., Napal, L., Rubin, T., Poidevin, M., Perrin, L., Wicker-Thomas, C.,
631 Montagne, J., 2012. Drosophila melanogaster Acetyl-CoA-carboxylase sustains a
632 fatty acid-dependent remote signal to waterproof the respiratory system. PLoS Genet
633 8, 30.
634 Piwko, P., Vitsaki, I., Livadaras, I., Delidakis, C., 2019. The Role of Insulators in
635 Transgene Transvection in Drosophila. Genetics,
636 genetics.302165.302019.
637 Qiu, Y., Tittiger, C., Wicker-Thomas, C., Le Goff, G., Young, S., Wajnberg, E.,
638 Fricaux, T., Taquet, N., Blomquist, G.J., Feyereisen, R., 2012. An insect-specific
639 P450 oxidative decarbonylase for cuticular hydrocarbon biosynthesis. Proc Natl Acad
640 Sci U S A 109, 14858-14863.
641 Tsakireli, D., Riga, M., Kounadi, S., Douris, V., Vontas, J., 2019. Functional
642 characterization of CYP6A51, a cytochrome P450 associated with pyrethroid
643 resistance in the Mediterranean fruit fly Ceratitis capitata. Pesticide Biochemistry and
644 Physiology.
645 Wicker-Thomas, C., Garrido, D., Bontonou, G., Napal, L., Mazuras, N., Denis, B.,
646 Rubin, T., Parvy, J.P., Montagne, J., 2015. Flexible origin of hydrocarbon/pheromone
647 precursors in Drosophila melanogaster. J Lipid Res 56, 2094-2101.
648 Wigglesworth, V.B., 1988. The source of lipids and polyphenols for the insect cuticle:
649 The role of fat body, oenocytes and oenocytoids. Tissue Cell 20, 919-932.

650

651

652

653

654

655

FIGURE CAPTIONS

657

Figure 1. Immunohistochemical localization of CYP4Gs. Merged immunohistochemical images from longitudinal sections of 4th instar mosquito larvae focusing on oenocytes. A) CYP4G17 peripheral localization in *An. gambiae* larval oneocytes, B) CYP4G16 peripheral localization in *An. gambiae* larval oenocytes. Cell nuclei are stained red with TOPRO; scale bars= 10μm. *Left*: bright-field with stained nuclei, *middle*: antibody and nuclei staining, *right*: merge of bright-field, antibody and nuclei staining.

665

Figure 2. Membrane topology of CYP4Gs. Immunohistochemical images from abdnominal walls (whole mounts) of 4th instar mosquito larvae focusing on oenocytes. A) CYP4G17 and B) CYP4G16 in permeabilized and non-permeabilized conditions; scale bars= 1mm.

670

Figure 3. Immunohistochemical localization of CYP4Gs in pupae. Merged immunohistochemical images from longitudinal sections of pupal abdominal walls. A) CYP4G16 localization in larval-origin pupal oenocytes mainly on the periphery of oenocytes, B) CYP4G16 localization in adult-origin pupal oenocytes mainly on the periphery, C) CYP4G17 localization in larval-origin pupal oenocytes mainly on the periphery of oenocytes, D) CYP4G17 localization in adult-origin, newly-developed oenocytes of pupae, forming a cluster, showing the protein dispersed throughout the cytoplasm. Cell nuclei are stained red with TOPRO; scale bars= 10μm.. *Left*: bright-field with stained nuclei, *middle*: antibody and nuclei staining, *right*: merge of bright-field, antibody and nuclei staining.

681

Figure 4. Expression pattern of CYP4G17 among different *An. gambiae* developmental stages. Whole protein extracts from dissected abdominal walls of 4th instar larvae (lane 1), newly-formed pupae (lane 2), pupae prior to emergence (lane 3)

22

685 and newly emerged adults (lane 4), were analyzed by western blot using anti-

686 CYP4G17.

687

688 **Figure 5. Percent eclosion of *D. melanogaster* flies in different CYP4G**

689 **backgrounds.** Quantification of adult flies that successfully eclosed corresponding to

690 a known number of pupae. White bars represent successfully eclosed adults that

691 survived (%), while flies that died as newly-emerged adults lying on the food were

692 calculated to address mortality post successful eclosion (%) and are depicted with

693 grey bars. Different CYP4G backgrounds are described at the bottom of the graph

694 with "+" representing the presence and "–" the absence of a P450 gene (*Cyp4g1*,

695 *CYP4G17*, *and CYP4G16*) or the oenocyte-specific GAL4 driver (REGal4). Mean of

696 3 biological experiments + SEM.

697

698 **Figure 6. Relative abundance of Cuticular Hydrocarbons (CHCs) identified in**

699 **different CYP4G backgrounds.** Relative CHCs abundances in % area are depicted

700 for each one of the 21 out of 32 CHCs identified in total. Differentially colored bars

701 correspond to the different CYP4G background present in each *Drosophila* strain

702 analyzed (grey: G x 1 , black: C x 3, white: B x 2 and black/white: B x 3 fly crosses

703 as described in Table S2). Mean of 3 biological experiments ± SEM.

Table S 1. Primer list: Names, IDs and sequences (5'-3') of all primer pairs used for cloning (c) and sequencing (s) of *An. gambiae* CYP4G ORFs.

Gene	ID	Primername	PrimerSequence (5'-3')
CYP4G16	AGAP001076-PA	*CYP4G16*F (c)	GCGCGCACCATGTCAGCAACAATTGCGCATACAG
		*CYP4G16*R (c)	CTCGAGTCATAATGTCTTCGATTTGCGTTGA
CYP4G17	AGAP000877	*CYP4G17*F (c)	GGCGCGCCCACCATGGGCATTGAAACGATCCC
		*CYP4G17*R (c)	GTCGACTCATGCCCTCGGCTCCAGCT
		pPel_uas F (s)	GAAGAGAACTCTGAATAGGGAATTG
		pPel_sv40 R (s)	CAAATGTGGTATGGCTGATTATG

Table S 2. Combinations of crosses for the constructions of all genotypes used for downstream experiments (eclosion and adult mortality estimation and phenotypic observation of flies and cuticular hydrocarbon analysis).

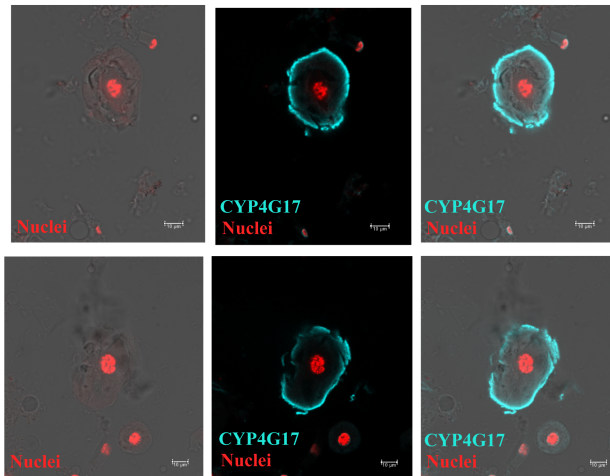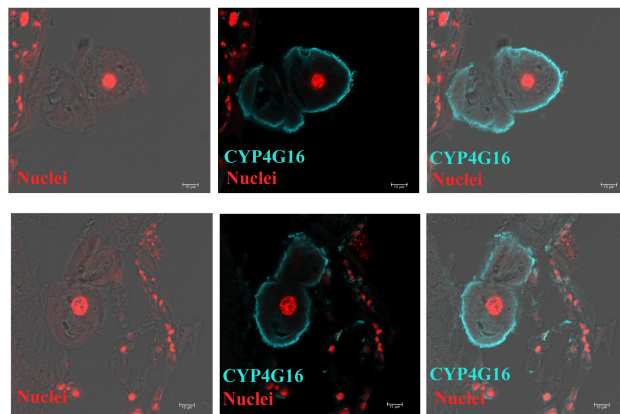| ♀ \ ♂	$\frac{REGal4}{REGal4};\frac{+}{+}$ **1**	$\frac{REGal4}{REGal4};\frac{UAS-CYP4G16}{UAS-CYP4G16}$ **2**	$\frac{REGal4}{REGal4};\frac{UAS-CYP4G17}{UAS-CYP4G17}$ **3**	$\frac{UAS-dsCyp4g1}{UAS-dsCyp4g1};\frac{UAS-CYP4G17}{UAS-CYP4G17}$ **4**
$\frac{UAS-dsCyp4g1}{UAS-dsCyp4g1};\frac{+}{+}$ **A**	$\frac{REGal4}{UAS-dsCyp4g1};\frac{+}{+}$	-	-	-
$\frac{UAS-dsCyp4g1}{UAS-dsCyp4g1};\frac{UAS-CYP4G16}{UAS-CYP4G16}$ **B**	$\frac{REGal4}{UAS-dsCyp4g1};\frac{UAS-CYP4G16}{+}$	$\frac{REGal4}{UAS-dscyp4g1};\frac{UAS-CYP4G16}{UAS-CYP4G16}$	$\frac{REGal4}{UAS-dsCyp4g1};\frac{UAS-CYP4G17}{UAS-CYP4G16}$	$\frac{UAS-dsCyp4g1}{UAS-dsCyp4g1};\frac{UAS-CYP4G17}{UAS-CYP4G16}$
$\frac{UAS-dsCyp4g1}{UAS-dsCyp4g1};\frac{UAS-CYP4G17}{UAS-CYP4G17}$ **C**	$\frac{REGal4}{UAS-dsCyp4g1};\frac{attB.UAS-CYP4G17}{+}$	$\frac{REGal4}{UAS-dsCyp4g1};\frac{UAS-CYP4G17}{attB.UAS-CYP4G16}$	$\frac{REGal4}{UAS-dsCyp4g1};\frac{UAS-CYP4G17}{UAS-CYP4G17}$	-
$\frac{REGal4}{REGal4};\frac{UAS-CYP4G17}{UAS-CYP4G17}$ **D**		$\frac{REGal4}{REGal4};\frac{UAS-CYP4G16}{UAS-CYP4G17}$	-	-
$\frac{+}{+};\frac{UAS-CYP4G16}{UAS-CYP4G16}$ **E**	-	$\frac{REGal4}{+};\frac{UAS-CYP4G16}{UAS-CYP4G16}$	-	-
$\frac{+}{+};\frac{UAS-CYP4G17}{UAS-CYP4G17}$ **F**	-		$\frac{REGal4}{+};\frac{UAS-CYP4G17}{UAS-CYP4G17}$	-
$\frac{+}{+};\frac{VK13}{VK13}$ **G**	$\frac{REGal4}{+};\frac{VK13}{+}$	-	-	-

Figure 1.

A

B
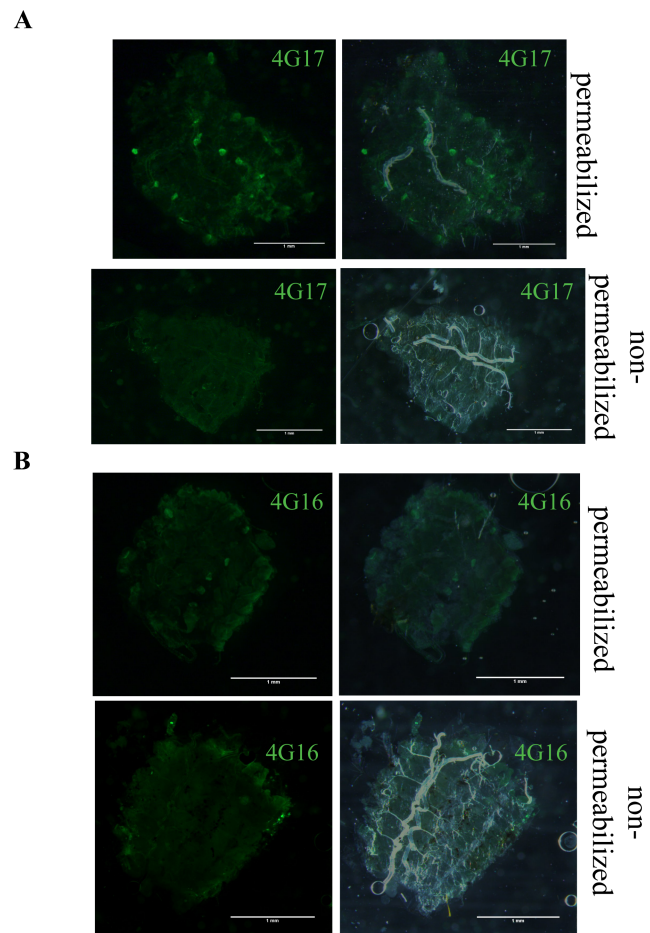
Figure 2.
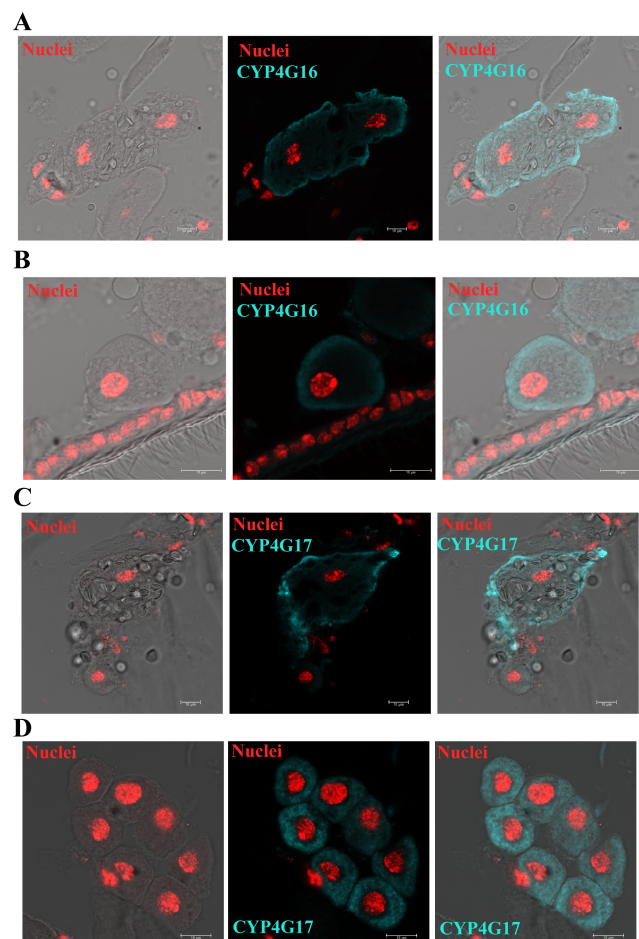
Figure 3.
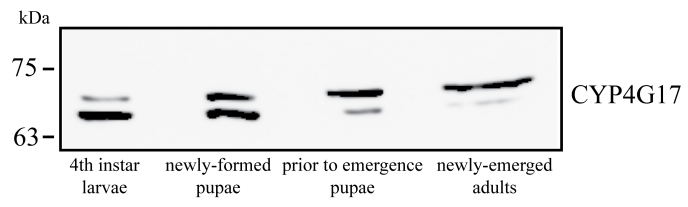
Figure 4.

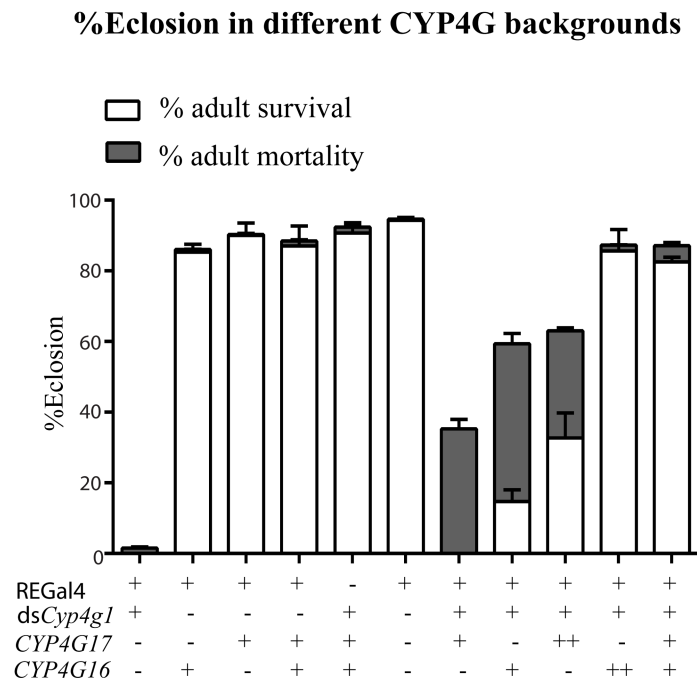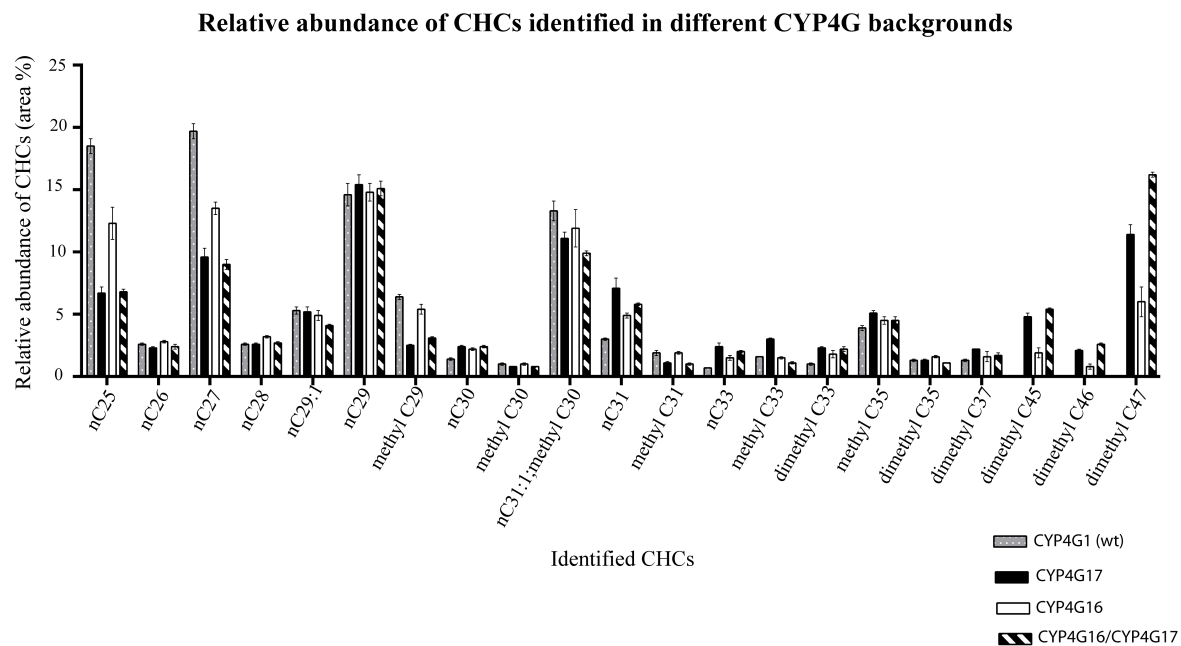## %Eclosion in different CYP4G backgrounds

Figure 5.

Figure 6.

Highlights

- ➢ The two *An. gambiae* CYP4Gs (CYP4G17 and CYP4G16) are localized on the cytoplasmic side of larval oenocyte plasma membrane.

- ➢ CYPG17 is differentially localized in two distinct types of pupal oenocytes, of larval and adult specificity.

- ➢ Both CYP4G16 and CYP4G17 rescue the adult lethal phenotype of *Cyp4g1-*KD flies, indicating CYP4G17 decarbonylase activity.

- ➢ CYP4G16 and CYP4G17 produce similar CHC profiles to CYP4G1, apart from three very long-chain dimethyl-branched CHCs.